Nuclear Physics B119 (1977) 515–538


# A SELECTION RULE ON ANGULAR MOMENTUM TRANSFER IN REACTIONS OF THE TYPE $0^- \frac{1}{2}^+ \to 1^- \frac{3}{2}^+$

Manuel G. DONCEL *, Louis MICHEL and Pierre MINNAERT **
*Institut des Hautes Etudes Scientifiques, 91440 Bures-sur-Yvette, France*

Received 9 August 1976

An analysis of 50 experimental data on polarization and correlations of polarization in the reactions $\pi N \to \rho\Delta$, $\omega\Delta$ and $KN \to K^*\Delta$, $\rho\Sigma^*$, $\Phi\Sigma^*$ strongly suggests a pure $\Delta J = 1$ transition at the baryon vertex. A plot for testing graphically the linear constraints of the selection rule $\Delta J = 1$ is proposed.

## 1. Introduction

The study of differential cross sections in high-energy physics has revealed simple and fundamental laws for the dependence on energy and on momentum transfer. Similarly since all these reactions involve spinning particles, the study of polarization effects may allow the discovery of simple and fundamental laws for the dependence on angular momentum transfer.

As an example of such a study we have analyzed all available data on polarization correlations in hadronic reactions of the type

$$0^- \tfrac{1}{2}^+ \to 1^- \tfrac{3}{2}^+ . \tag{1}$$

While the change of spin at the baryon vertex could be obtained by both angular momentum transfers $\Delta J = 1$ and $\Delta J = 2$, we find that the experimental data strongly suggest a pure $\Delta J = 1$ transition. It would be very worthwhile to check whether this selection rule $\Delta J = 1$ is valid in other hadronic reactions in which a baryon jumps from the $\frac{1}{2}^+$ octet to the $\frac{3}{2}^+$ decuplet (just as for instance the $\Delta I = \frac{1}{2}$ rule has been well established in all semi-leptonic decays with change of strangeness).

Reactions of type (1) are among the most complicated polarization measurements currently performed in high-energy physics: at least 19 significant polarization parameters can be measured. In a communication to the second Aix-en-Provence Conference [1] we proposed a rather powerful test of the rule $\Delta J = 1$, using only three polarization parameters, corresponding to the joint polar angle decay distribution of

* Departamento de Física Teórica, Universidad Autónoma de Barcelona Bellaterra (Barcelona), Spain
** Laboratoire de Physique Théorique, Université Bordeaux I, Gradignan 33170, France.

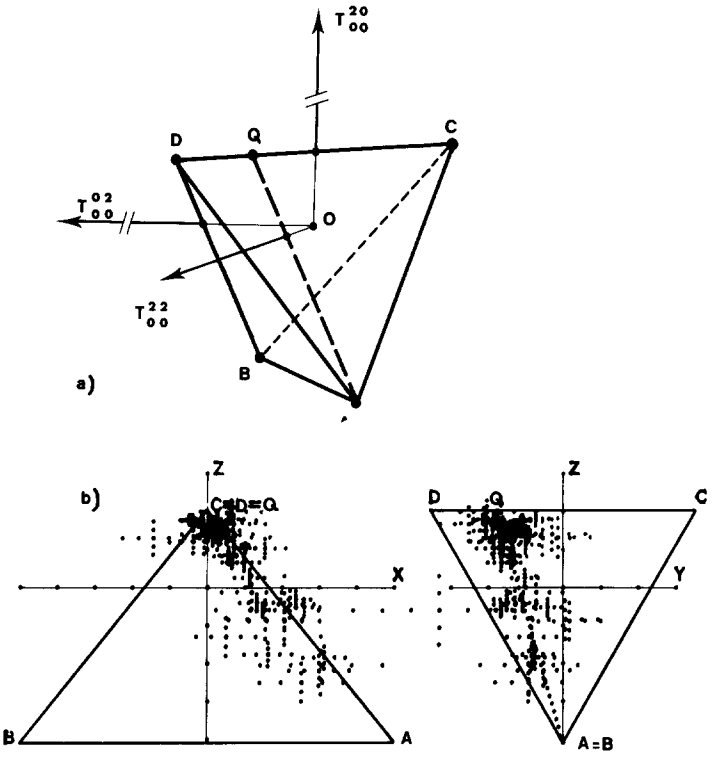


Fig. 1. (a) Polarization domain of joint polarization for particles with spin 1 and $\frac{3}{2}$ for the space $\mathcal{C}_D$ of the three measurable diagonal parameters of the joint density matrix. The prediction of the rule $\Delta J = 1$ is the segment $AQ$ in the face $ACD$ of the tetrahedron. Note that opposite edges of the tetrahedron are orthogonal. (b) The two triangles are projections of the tetrahedron on the two orthogonal planes orthogonal to the edges $CD$ and $AB$ respectively. If a point is inside the two triangles it is inside the tetrahedron. We have plotted all the data available in the literature (50 measurements). In order not to emphazise data with large errors, instead of darwing a full cross of errors for each point, we plot only 9 points on each cross.

the final resonances in transversity quantization. We present this test in fig. 1 for all data we found in the literature. The three polarization parameters are the coordinates of a point in a 3-dimensional polarization space. By angular momentum and parity conservation the experimental points should be inside the polarization domain which is the tetrahedron $ABCD$. The selection rule $\Delta J = 1$ predicts that these points should lie on the line segment $AQ$ in the face $ACD$, with $Q$ on the edge $CD$. The agreement of the 50 experimental points with the predictions of the rule is quite spectacular *.

* In order to show that the effect is a real one we have plotted the same parameters in helicity quantization. In that case the rule $\Delta J = 1$ implies no relation between the parameters and indeed the experimental points are not clustered, they fill a large domain in the tetrahedron.

In this paper we present a more complete graphical test of the rule $\Delta J = 1$, using seven polarization parameters instead of three. In sect. 2 we give some general considerations on the tests of theoretical predictions by polarization measurements. In sect. 3 we recall how the polarization observables of reaction (1) are measured and we give their relations with the transversity amplitudes. In sect. 4 we discuss the selection rule $\Delta J = 1$, its predictions for the transversity amplitudes and for the polarization observables and we propose a plot for testing the linear constraints predicted by the rule. Sect. 5 is devoted to a test of the rule against all the data found in the literature.

Before going to the body of the paper we would like to mention that the selection rule $\Delta J = 1$ is contained in some more specific models. For instance the Stodolsky-Sakurai model [2] for the reactions $0^- \frac{1}{2}^+ \to 0^- \frac{3}{2}^+$ implies $\Delta J = 1$, since it assumes that the reaction is dominated by the M1 transition. Similarly it is well known that the quark model [3–7] implies the $\Delta J = 1$ rule for all reactions with a transition from the $\frac{1}{2}^+$ octet to the $\frac{3}{2}^+$ decuplet. Indeed in this model the quarks are in an S state and the spin change from $\frac{1}{2}^+$ to $\frac{3}{2}^+$ during the collision is only due to the spin flip of one of the quarks and the spin flip of spin $\frac{1}{2}$ particle creates a pure $\Delta J = 1$ angular momentum transfer.

## 2. How to test theoretical predictions by polarization measurements

Every measurement procedure relies on some universally accepted first principles. Such data, i.e., the measures with their errors, can be used only to test the predictions of a theory which respects these first principles. Strictly speaking, theories (or models, or rules) can never be proven. They are only disproved whenever their predictions disagree with experimental data. However, the confidence in a theory will grow with the number of its experimental verifications.

Polarization measurements provide a good example of this situation. The $N$ observed polarization parameters of a particle or a set of particles form an $N$-dimensional Euclidean space, the polarization space $\mathcal{E}_N$. First principles as angular-momentum or parity conservation define a domain $\mathcal{D}$ in $\mathcal{E}_N$, the polarization domain *. The result of a polarization measurement is one (or several) points $E$ with its ellipsoid of errors $\Delta E$. The size of $\Delta E$ with respect to that of $\mathcal{D}$ is an evaluation of the precision of the measurement.

A theory (or a model or a rule) which respects the first principles defines a domain $\mathcal{D}_T$ in $\mathcal{D}$. The smaller $\mathcal{D}_T$ is compared to $\mathcal{D}$, the more predictive is the theory. A quantitative test of the theory can be made by a $\chi^2$-calculation. A simple geometrical evaluation consists in the comparison of the distance $ET$, from the experimental point $E$ to its nearest point $T$ of $\mathcal{D}_T$, with the size $\Delta_{ET}$ of the error in the direction

* The geometrical description of polarization is exposed in several papers [8–10]. For the unfamiliar readers we have summarized the main ideas in appendix A.

$ET$. If $E$ is in $\mathcal{D}_T$, $ET = 0$ and the predictions of the theory are perfectly satisfied. In general, the agreement will be considered good if the distance $ET$ is of the same order of magnitude as the error $\Delta_{ET}$. Of course, this comparison is meaningless if the measurement is not precise enough *.

In general the statistics of reaction (1) is too poor for measuring the polarization at sharp values of the momentum transfer $t$. The data is integrated over large bins in $t$ and sometimes it is summed over several values of the beam energy, i.e. of the invariant $s$. The experimental point $E$ which results from all these summations is the barycenter of the points $E(s, t)$ for the given values of the kinematical invariants. In that case the domain $\mathcal{D}_T$ must be replaced by the set of barycenters of points of $\mathcal{D}_T$, i.e. by its convex hull $\hat{\mathcal{D}}_T$ which is larger than $\mathcal{D}_T$ when the later is not convex. In this paper we shall consider a slightly poorer test since we shall replace the domain $\mathcal{D}_T$ by the intersection with $\mathcal{D}$ of the smallest linear manifold $\mathcal{E}_T$ which contains it. This corresponds to considering only the linear constraints between observables predicted by the theory, as they are invariant by integration in polarization space. This procedure was first proposed in ref. [5] for testing the predictions of the quark model.

## 3. Polarization observables in reactions of type (1)

For most hadronic reactions of type (1), the final resonances undergo two-body decays of the type

$$1^- \to 0^- 0^- , \qquad \tfrac{3}{2}^+ \to \tfrac{1}{2}^+ 0^- . \tag{2}$$

Polarizations and correlations of polarization are measured by observing the joint decay of the resonances with respect to some orthonormal bases: $(x, y, z)$ for the meson and $(x', y', z')$ for the baryon. We denote by $\Omega \equiv (\theta, \varphi)$ the polar and azimuthal angles of a specified spin-0 meson emitted by the vector meson ** and by $\Omega' \equiv (\theta', \varphi')$ the angles of the spin-0 meson emitted by the baryon ***. The joint angular distribution $I(\theta, \varphi, \theta', \varphi')$ is characterized by its moments

$$y_{MM'}^{LL'} = \langle Y_M^L(\Omega) Y_{M'}^{L'}(\Omega') \rangle , \tag{3}$$

* If for instance the size of $\Delta_E$ turns out to be of the same order as that of $\mathcal{D}$ then nothing is measured and the experiment will be in good agreement with any prediction $\mathcal{D}_T$. For such an example see ref. [11].

** For the three-body decay $1^- \to 0^- 0^- 0^-$ (e.g. $\omega^0 \to \pi^+ \pi^- \pi^0$) the angles $\Omega \equiv (\theta, \varphi)$ are those of the normal to the decay plane.

*** The baryon may undergo a sequential decay, for instance $\Sigma^* \to \Lambda\pi$, $\Lambda \to p\pi$. In this case because of parity violation in the decay of the $\Lambda$ an analysis of the sequential decay angular distribution yields more information on the polarization of the final state, see refs. [12,13] We do not consider this case here since the data is meager.

which satisfy the identities (the bar means complex conjugation)

$$\overline{y^{LL'}_{MM'}} = (-1)^{M+M'} y^{LL'}_{-M-M'} . \tag{4}$$

By angular momentum and parity conservation in the decays (2) the only non-vanishing moments are those with

$$L = 0, 2 , \qquad L' = 0, 2 . \tag{5}$$

Transversity bases are defined by choosing the third axes $z$ and $z'$ along the normal to the reaction plane of (1). In such bases the conditions on the moments (3) imposed by parity conservation in reaction (1) are easily expressed. They read

$$y^{LL'}_{MM'} = 0 \qquad \text{if } M + M' \text{ is odd} . \tag{6}$$

To define completely the transversity bases one must also choose the first axes $x$ and $x'$ which fix the origin of the azimuthal angles $\varphi$ and $\varphi'$. We shall not discuss this choice here since the simplified test described in ref. [1] and the more complete test proposed here are independent of this choice.

Once transversity bases are defined and after conditions (4), (5) and (6) are imposed there remains 19 linearly independent real quantities to determine *. Even though they measure the real and imaginary parts of the moments $y^{LL'}_{MM'}$, most experimentalists prefer to publish the values of some set of parameters which are either proportional to the moments (e.g. the multipole parameters $T^{LL'}_{MM'}$) or linear combinations of the moments (e.g. the joint density matrix elements $\rho^{\mu\mu'}_{\nu\nu'}$ or the $R$ and $U$ parameters) **. In part (a) of table 1 we recall *** the relations between the moments $y^{LL'}_{MM'}$, the multipole parameters $T^{LL'}_{MM'}$ and the density matrix elements $\rho^{\mu\mu'}_{\nu\nu'}$.

Hence the polarization observables for reactions of type (1) form a 19-dimensional Euclidean space $\mathcal{E}_{19}$. A set of orthonormal parameters $(p_i, i = 1, ..., 19)$ for this space is given by the real multipole parameters $T^{LL'}_{00}$ and the real and imaginary parts of the parameters $\sqrt{2}\, T^{LL'}_{MM'}$ with $M$ and/or $M' \neq 0$, cf. appendix A. We have no closed form for the equations of the boundary of the observed polarization domain $\mathcal{D}$ in terms of these parameters. However, we can give the equations of the projections of $\mathcal{D}$ on some low dimensional $k$-planes in $\mathcal{E}_{19}$, cf. sect. 4 and appendix C.

* If those moments $y^{LL'}_{MM'}$ which are expected to vanish do not, it means that the experiment cannot be simply interpreted in terms of pure resonances non interfering with the background. In this case the test we propose is irrelevant.

** We want to point out the irony of the actual situation. All experimentalists, as far as we know, had first obtained the moments $y^{LL'}_{MM'} = \langle Y^L_M Y^{L'}_{M'} \rangle$ from their data, before tranforming them into their pet system of parameters, ($T^{LL'}_{MM'}$, $\rho^{\mu\mu'}_{\nu\nu'}$, $R$ and $U$, etc ...). So, for using their data, we had to write the programs making all the inverse transformations. How much simpler it would be if the $y^{LL'}_{MM'}$ would be published by all. (Some experimental papers discuss their data, e.g. in figures, without even publishing it).

*** For a proof of all these relations see refs. [8,13].

Table 1
Observables of the reaction $0^{-}\frac{1}{2}^{+} \to 1^{-}\frac{3}{2}^{+}$ in terms of the transversity amplitudes

(a) Relations between the moments and the polarization parameters

$$4\pi y^{LL'}_{MM'} = C(L)C'(L')2\sqrt{3}[(2L+1)(2L'+1)]^{-1/2}T^{LL'}_{MM'}$$

$$= C(L)C'(L') \sum_{\mu,\mu',\nu,\nu'} \langle 1\mu LM|1\nu\rangle\langle \tfrac{3}{2}\mu' L'M'|\tfrac{3}{2}\nu'\rangle \rho^{\mu\mu'}_{\nu\nu'}$$

with $C(0) = C'(0) = 1$, $\quad C(2) = -\sqrt{2}$, $\quad C'(2) = -1$.

(b) Transversity amplitudes

| $\lambda = \frac{1}{2}$ | $\lambda = -\frac{1}{2}$ | $\mu\mu'$ | |
|---|---|---|---|
| $e$ | 0 | $\frac{3}{2}$ | |
| 0 | $c'$ | $\frac{1}{2}$ | 1 |
| $b$ | 0 | $-\frac{1}{2}$ | |
| 0 | $f'$ | $-\frac{3}{2}$ | |
| 0 | $d'$ | $\frac{3}{2}$ | |
| $a$ | 0 | $\frac{1}{2}$ | 0 |
| 0 | $a'$ | $-\frac{1}{2}$ | |
| $d$ | 0 | $-\frac{3}{2}$ | |
| $f$ | 0 | $\frac{3}{2}$ | |
| 0 | $b'$ | $\frac{1}{2}$ | −1 |
| $c$ | 0 | $-\frac{1}{2}$ | |
| 0 | $e'$ | $-\frac{3}{2}$ | |

$A^{\mu\mu'}_{\lambda} =$

$$\sigma\rho^{\mu\mu'}_{\nu\nu'} = \frac{1}{2}\sum_{\lambda} A^{\mu\mu'}_{\lambda}\overline{A^{\nu\nu'}_{\lambda}}$$

$$\sigma = \frac{1}{2}\sum_{\mu\mu'\lambda} |A^{\mu\nu}_{\lambda}|^2$$

(c) Relation between observables and amplitudes

$$2\sigma = \Delta_A + \Delta_B + \Delta_C + \Delta_D$$

$$T^{02}_{00} = (1/\sqrt{12})(-\Delta_A + \Delta_B - \Delta_C + \Delta_D)/2\sigma$$

$$T^{22}_{00} = (1/\sqrt{24})(2\Delta_A - 2\Delta_B - \Delta_C + \Delta_D)/2\sigma$$

$$T^{20}_{00} = (1/\sqrt{24})(-2\Delta_A - 2\Delta_B + \Delta_C + \Delta_D)/2\sigma$$

$$\sqrt{2}\,T^{02}_{02} = (1/\sqrt{3})(\langle d|a\rangle + \langle b|e\rangle + \langle c|f\rangle)/2\sigma$$

$$\sqrt{2}\,T^{22}_{02} = (1/\sqrt{6})(-2\langle d|a\rangle + \langle b|e\rangle + \langle c|f\rangle)/2\sigma$$

$$\sqrt{2}\,T^{22}_{20} = (1/\sqrt{2})(\langle f|e\rangle - \langle c|b\rangle)/2\sigma$$

$$\sqrt{2}T^{20}_{20} = (1/\sqrt{2})(\langle f|e\rangle + \langle c|b\rangle)/2\sigma$$

$$\sqrt{2}\,T^{22}_{22} = \langle c|e\rangle/2\sigma$$

$$\sqrt{2}\,T^{22}_{2-2} = \langle b|f\rangle/2\sigma$$

$$\sqrt{2}\,T^{22}_{11} = (1/\sqrt{2})(\langle a|e\rangle - \langle d|b\rangle)/2\sigma$$

$$\sqrt{2}\,T^{22}_{1-1} = (1/\sqrt{2})(\langle a|f\rangle - \langle d|c\rangle)/2\sigma$$

*Notation*

$$\Delta_A = \langle a|a\rangle, \quad \Delta_B = \langle d|d\rangle, \quad \Delta_C = \langle b|b\rangle + \langle c|c\rangle,$$

$$\Delta_D = \langle e|e\rangle + \langle f|f\rangle,$$

$$\langle X|Y\rangle = X\overline{Y} + \overline{X}'Y' \quad (X, Y = a, b, c, d, e, f)$$

The set of amplitudes for reaction (1) form a 12 × 2 transition matrix:

$$A^{\mu\mu'}_{\lambda}; \qquad \mu = 1, 0, -1, \qquad \mu' = \tfrac{3}{2}, \tfrac{1}{2}, -\tfrac{1}{2}, -\tfrac{3}{2}, \qquad \lambda = \tfrac{1}{2}, -\tfrac{1}{2}. \tag{7}$$

In transversity bases for initial and final particles, parity conservation implies

$$A^{\mu\mu'}_{\lambda} = 0 \qquad \text{for } \mu + \mu' - \lambda \quad \text{odd}. \tag{8}$$

Table 1b gives an explicit nomenclature for the 12 non-vanishing complex amplitudes. As in ref. [14] the amplitudes with $\lambda = -\frac{1}{2}$ are called $a, b, c, d, e, f$, those with $\lambda = +\frac{1}{2}$ are called $a', b', c', d', e', f'$.

At fixed values of $s$ and $t$ the joint density matrix $\rho_f$ of the final particles is deduced from the transition matrix $A$ and the initial polarization density matrix $\rho_i$ by the general equation

$$\sigma\rho_f = A\rho_i A^+ , \tag{9}$$

where $\sigma$ is the differential cross section. For unpolarized initial particles $\rho_i$ is the $2 \times 2$ matrix $\frac{1}{2}$ **1**. The explicit relation between the matrix elements of $\rho_f$ and those of $A$ is written in table 1b. From this equation one deduces the relations between the joint multipole parameters $T^{LL'}_{MM'}$ and the amplitudes. They are given in table 1c. Because of the summation over $\lambda$, the amplitudes contribute to the observables through combinations of the type

$$\langle x|y\rangle = x\bar{y} + \bar{x}'y' . \tag{10}$$

Eq. (10) can be considered as the hermitian product of the 2-dimensional vectors $|x\rangle$ and $|y\rangle$ defined by

$$|x\rangle = \begin{pmatrix} \bar{x} \\ x' \end{pmatrix} , \qquad |y\rangle = \begin{pmatrix} \bar{y} \\ y' \end{pmatrix} . \tag{11}$$

Since this hermitian scalar product is invariant for any transformation of the unitary group U(2) (a 4-parameter group) only 20 of the 24 real amplitudes are effective degrees of freedom *. Furthermore at fixed value of the differential cross section $\sigma$,

$$\sigma = \langle a|a\rangle + \langle b|b\rangle + \langle c|c\rangle + \langle d|d\rangle + \langle e|e\rangle + \langle f|f\rangle , \tag{12}$$

the 19 polarization parameters depend on 19 degrees of freedom. Consequently the "amplitude domain" $\mathcal{D}_A$ allowed for the polarization parameters by eq. (9) has the same dimension as the polarization space. It has been shown [16,17] that the domain $\mathcal{D}_A$ is not convex and hence it is smaller than $\mathcal{D}_{ob}$, but its convex hull $\hat{\mathcal{D}}$ is equal to $\mathcal{D}$ .

## 4. Predictions of the rule $\Delta J = 1$

Let us denote by $A^{\mu'}_{\lambda}$ the $4 \times 2$ transition matrix between the spin spaces of the baryons, for any value of the quantum number $\mu$ of the final meson ($\mu = 1, 0, -1$).

* This means that there is a U(2) ambiguity in the reconstruction of the amplitudes from a study of the final state. Such ambiguities were pointed out by Simonius [15] and are studied in more details in refs. [14,16].

For any rotation $R$ of the bases for the baryons the transition matrix $A$ is transformed into ${}^{R}A$ according to

$$({}^{R}A)_{l}^{m'} = D^{3/2}(R)_{\mu}^{m'} A_{\lambda}^{\mu'} D^{1/2}(R)_{l}^{\dagger\lambda} . \tag{13}$$

We denote by $\widetilde{A}$ the $8 \times 1$ matrix deduced from $A$ by transposition in the column index, i.e.,

$$\widetilde{A}^{\lambda\mu'} = A_{\lambda}^{\mu'} . \tag{14}$$

In the rotation $R$ this matrix transforms as

$$({}^{R}\widetilde{A})^{lm'} = \overline{D^{1/2}(R)_{\lambda}^{l}} D^{3/2}(R)_{\mu}^{m'} \widetilde{A}^{\lambda\mu'} , \tag{15}$$

or

$${}^{R}\widetilde{A} = (\overline{D^{1/2}(R)} \otimes D^{3/2}(R))\widetilde{A} . \tag{16}$$

It is well known that the representation $D^{j}$ and its complex conjugate $\overline{D^{j}}$ are equivalent. In particular one has

$$D^{1/2} = \Gamma \overline{D^{1/2}} \Gamma^{-1} , \qquad \text{with } \Gamma = \begin{pmatrix} 0 & 1 \\ -1 & 0 \end{pmatrix} . \tag{17}$$

Therefore, from eqs. (16) and (17), one has

$$(\Gamma \otimes \mathbb{1})^{R}\widetilde{A} = (D^{1/2} \otimes D^{3/2})(\Gamma \otimes \mathbb{1})\widetilde{A} , \tag{18}$$

i.e., the amplitudes in the matrix $(\Gamma \otimes \mathbb{1})\widetilde{A}$ are transformed under rotation by the direct product $D^{1/2} \otimes D^{3/2}$ whose reduction formula is

$$D^{1/2} \otimes D^{3/2} \sim D^{1} \otimes D^{2} . \tag{19}$$

Thus the transition matrix between the spin spaces of the baryons can be split into two parts which transform according to the representations $D^{1}$ and $D^{2}$ respectively. The selection rule $\Delta J = 1$ at the baryon vertex is expressed by imposing that the part which is transformed by $D^{2}$ vanishes.

The consequences of this rule for the transversity amplitudes in table 1b can be computed explicitly from the Clebsch-Gordan expansion

$$|\tfrac{1}{2}\lambda\rangle \otimes |\tfrac{3}{2}\mu'\rangle = \sum_{J=1,2} \sum_{M} \langle \tfrac{1}{2}\lambda \tfrac{3}{2}\mu | JM \rangle \, |JM\rangle . \tag{20}$$

For $\mu = 0$ and 1 one gets, respectively,

$$(\Gamma \otimes 1)\widetilde{A} = d'|22\rangle + \sqrt{\tfrac{1}{2}}\,(a' - a)|20\rangle - d|2 - 2\rangle + \sqrt{\tfrac{1}{2}}\,(a' + a)|10\rangle , \tag{21a}$$

$$(\Gamma \otimes 1)\widetilde{A} = \tfrac{1}{2}(\sqrt{3}\,c' - e)|21\rangle + \tfrac{1}{2}(f' - \sqrt{3}\,b)|2-1\rangle$$
$$+ \tfrac{1}{2}(c' + \sqrt{3}\,e)|11\rangle + \tfrac{1}{2}(\sqrt{3}\,f' + b)|1-1\rangle\,. \qquad (21b)$$

The corresponding equation for $\mu = -1$ is deduced from eq. (21b) by the substitutions $c' \to b', f' \to e', b \to c$ and $e \to f$. Therefore the rule $\Delta J = 1$ (i.e., the requirement that the coefficients of the vectors $|2M\rangle$ should vanish) yields seven complex conditions between the 12 amplitudes, cf. table 2a,

$$d = d' = 0\,, \qquad \sqrt{3}\,b = f'\,, \qquad \sqrt{3}\,c = e'\,, \qquad (22)$$
$$a = a'\,, \qquad \sqrt{3}\,c' = e\,, \qquad \sqrt{3}\,b' = f\,,$$

and leaves five linearly independent non-vanishing amplitudes $a, b, b', c, c'$.

We now turn to the relations between the polarization observables implied by the conditions (22). Using table 1c it is easy to write the 19 quantities $\sigma T^{LL'}_{MM'}$ in terms of the amplitudes $a, b, b', c, c'$, see eq. (B.2). Since the observables are independent of the overall phase of the amplitudes, at fixed values of the differential cross section $\sigma$,

$$\sigma = |a|^2 + 2|b|^2 + 2|b'|^2 + 2|c'|^2\,, \qquad (23)$$

the number of degrees of freedom is 8. Thus the 19 multipole parameters must satisfy 11 constraints. These constraints are written explicitly in appendix B. Six of them are linear, see eq. (B.3); they are the class A conditions of the quark model [5]. The five other constraints are of higher degree, eq. (B.6), (B.8).

Since there are six linear constraints, the domain $\mathcal{D}_T$ predicted by the rule $\Delta J = 1$ is contained in a 13-plane $\mathcal{C}_T$ of the polarization space $\mathcal{C}_{19}$. According to the general considerations in sect. 1, for the present experimental data, we shall only check the rule $\Delta J = 1$ against the linear conditions (B.3) which are invariant by integration in the polarization space. For this we must parametrize the 6-plane $\mathcal{C}_P$ orthogonal to the plane $\mathcal{C}_T$. It is interesting to consider in $\mathcal{C}_P$ three mutually orthogonal 2-planes parametrized by the coordinates $(X_1, Y_1), (X_2, Y_2)$ and $(X_3, Y_3)$, respectively. Table 2b shows explicitly the orthogonal transformation which relates these parameters to the multipole parameters. By the orthogonal projection on $\mathcal{C}_P$ the whole subspace $\mathcal{C}_T$ is projected on the point $T_P$, cf. table 2c,

$$X_1 = -\sqrt{\tfrac{2}{105}}\,, \qquad Y_1 = \sqrt{\tfrac{1}{60}}\,, \qquad X_2 = 0 = Y_2\,, \qquad X_3 = 0 = Y_3\,. \qquad (24)$$

Let $E_P$ be the projection of the experimental point $E$ on $\mathcal{C}_P$. The distance $E_P T_P$ gives directly the discrepancy between the data and the theoretical prediction.

In ref. [1] we considered a 3-plane $\mathcal{C}_D$ parametrized by the coordinates $(X, Y, Z)$ defined in table 2b. The intersection of this 3-plane with $\mathcal{C}_P$ is the 2-plane $(X_1, Y_1)$. We call $Z_1$ the third orthogonal coordinate in $\mathcal{C}_D$. The projection of the polar-

Table 2
Test of the selection rule $\Delta J = 1$

(a) Relations between the transversity amplitudes in table 1, imposed by the rule $\Delta J = 1$

$$a = a' , \quad d = d' = 0 , \quad e = \sqrt{3}\, c' , \quad e' = \sqrt{3}\, c , \quad f = \sqrt{3}\, b' , \quad f' = \sqrt{3}\, b$$

(b) Orthogonal transformation which defines the coordinates

$$Z = T_{00}^{20}$$

$$X = -\sqrt{\tfrac{1}{3}}\, T_{00}^{02} + \sqrt{\tfrac{2}{3}}\, T_{00}^{22}$$

$$Y = -\sqrt{\tfrac{2}{3}}\, T_{00}^{02} - \sqrt{\tfrac{1}{3}}\, T_{00}^{22}$$

$$Z_1 = \sqrt{\tfrac{2}{7}}\, T_{00}^{02} - \sqrt{\tfrac{1}{7}}\, T_{00}^{22} + \sqrt{\tfrac{4}{7}}\, T_{00}^{20}$$

$$X_1 = -\sqrt{\tfrac{18}{35}}\, T_{00}^{02} - \sqrt{\tfrac{16}{35}}\, T_{00}^{22} + \sqrt{\tfrac{1}{35}}\, T_{00}^{20}$$

$$Y_1 = -\sqrt{\tfrac{1}{5}}\, T_{00}^{02} + \sqrt{\tfrac{2}{5}}\, T_{00}^{22} + \sqrt{\tfrac{2}{5}}\, T_{00}^{20}$$

$$X_2 + iY_2 = -\sqrt{\tfrac{1}{5}}\, (\sqrt{2}\, T_{20}^{20}) - \sqrt{\tfrac{4}{5}}\, (\sqrt{2}\, T_{20}^{22})$$

$$X_3 + iY_3 = \sqrt{\tfrac{1}{3}}\, (\sqrt{2}\, T_{02}^{02}) - \sqrt{\tfrac{2}{3}}\, (\sqrt{2}\, T_{02}^{22})$$

(c) Linear constraints implied by (a)

$$X_1 = -\sqrt{\tfrac{2}{105}} , \qquad Y_1 = \sqrt{\tfrac{1}{60}} , \qquad X_2 = Y_2 = X_3 = Y_3 = 0$$

(d) Coordinates of the tetrahedron vertices $A, B, C, D$ and of the point $Q$, in the 3-plane $XYZ$ or $X_1 Y_1 Z_1$

| | $(X$ | $Y$ | $Z)$ | $(X_1$ | $Y_1$ | $Z_1)$ |
|---|---|---|---|---|---|---|
| $A =$ | $(\tfrac{1}{2},$ | $0,$ | $-\sqrt{\tfrac{1}{6}})$ | $= (-\sqrt{\tfrac{2}{105}},$ | $\sqrt{\tfrac{1}{60}},$ | $-4\sqrt{\tfrac{1}{42}})$ |
| $B =$ | $(-\tfrac{1}{2},$ | $0,$ | $-\sqrt{\tfrac{1}{6}})$ | $= (\quad 0 \quad ,$ | $-5\sqrt{\tfrac{1}{60}},$ | $0\ )$ |
| $C =$ | $(\ 0,$ | $\sqrt{\tfrac{1}{8}},$ | $\tfrac{1}{2}\sqrt{\tfrac{1}{6}})$ | $= (\tfrac{11}{4}\sqrt{\tfrac{2}{105}},$ | $\sqrt{\tfrac{1}{60}},$ | $\tfrac{1}{2}\sqrt{\tfrac{1}{42}})$ |
| $D =$ | $(\ 0,$ | $-\sqrt{\tfrac{1}{8}},$ | $\tfrac{1}{2}\sqrt{\tfrac{1}{6}})$ | $= (-\tfrac{9}{4}\sqrt{\tfrac{2}{105}},$ | $\sqrt{\tfrac{1}{60}},$ | $\tfrac{3}{2}\sqrt{\tfrac{1}{42}})$ |
| $Q =$ | $(\ 0,$ | $-\tfrac{1}{2}\sqrt{\tfrac{1}{8}},$ | $\tfrac{1}{2}\sqrt{\tfrac{1}{6}})$ | $= (-\sqrt{\tfrac{2}{105}},$ | $\sqrt{\tfrac{1}{60}},$ | $\tfrac{5}{4}\sqrt{\tfrac{1}{42}})$ |

(e) Projections of the polarization domain $\mathcal{D}$ on the 2-planes $X_2 Y_2$ and $X_3 Y_3$

$$X_2^2 + Y_2^2 \leqslant \tfrac{9}{40} , \qquad X_3^2 + Y_3^2 \leqslant \tfrac{1}{4}$$

(f) Projections of the intersection of $\mathcal{D}$ by the plane $X_1 = -\sqrt{\tfrac{2}{105}}$, $Y_1 = \sqrt{\tfrac{1}{60}}$, $Z_1 = (\tfrac{21}{4} l - 4)\sqrt{\tfrac{1}{42}}$ $(l_A = 0, l_Q = 1)$

$$X_2^2 + Y_2^2 \leqslant \tfrac{9}{160}\, l^2 , \qquad X_3 = Y_3 = 0$$

ization domain $\mathcal{D}$ on this plane is a tetrahedron $ABCD$. The projections of the tetrahedron on the 2-planes $(X, Z)$ and $(Y, Z)$ are triangles. The prediction of the rule $\Delta J = 1$ is the projection of $\mathcal{E}_T$ on $\mathcal{E}_D$ in $\mathcal{D}$; this is a line segment $AQ$ lying in the face $ACD$ of the tetrahedron with $Q$ on the edge $CD$. The coordinates $(X, Y, Z)$ and $(X_1, Y_1, Z_1)$ of the vertices $A, B, C, D$ and of the point $Q$ are given in table 2d.

The plot we propose here for testing the linear constraints of the selection rule $\Delta J = 1$ consists of five figures corresponding to the five 2-planes $(X, Z)$, $(Y, Z)$, $(X_1, Y_1)$, $(X_2, Y_2)$ and $(X_3, Y_3)$, see fig. 2.

Under rotations (by the angles $\psi$ and $\psi'$ around the normal to the reaction plane) of the transversity bases for the final meson and baryon, the multipole parameters $T^{LL'}_{MM'}$ transform as

$$T^{LL'}_{MM'} \to e^{i(M\psi + M'\psi')} T^{LL'}_{MM'} . \tag{25}$$

Therefore the projections of the experimental points in the 2-planes $(X, Z)$, $(Y, Z)$ and $(X_1, Y_1)$ are invariant, while their projections in the 2-planes $(X_2, Y_2)$ and $(X_3, Y_3)$ are rotated by the angles $2\psi$ and $2\psi'$, respectively. This does not affect the linear predictions of the selection rule $\Delta J = 1$. They are independent of the choice of the transversity frames (e.g., $t$-channel or $s$-channel transversity frames or Donohue-Hogassen frames, for the meson or for the baryon or for both final particles). The plots drawn in sect. 5 for checking the rule $\Delta J = 1$ use data measured in $t$-channel transversity bases for both particles.

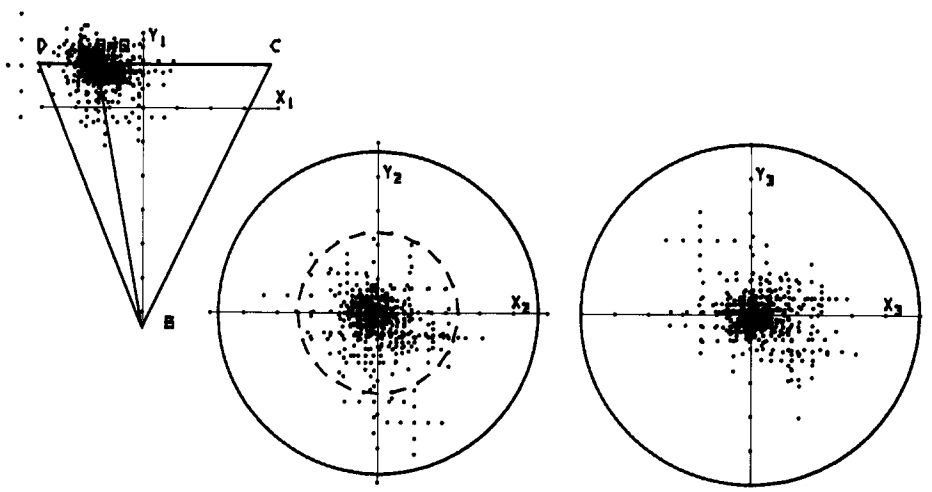


Fig. 2. Projections of the polarization domain on the three 2-planes $(X_1, Y_1)$, $(X_2, Y_2)$, $(X_3, Y_3)$ which span $\mathcal{E}_P$. The selection rule $\Delta J = 1$ predicts the point $T_P$ whose projections are respectively the point $A = Q$ and the centers of the circles. We have plotted the same experimental events as in fig. 1b. If the experimental points is projected on $A = Q$ in $(X_1 Y_1)$, then by angular momentum and parity conservation its other projections must be inside the dotted circle in $(X_2 Y_2)$ and at the origin of $(X_3 Y_3)$.

Although the proposed "tetrahedron test" of ref. [1] was very predictive ($AQ$ is a line segment in a three dimensional domain) it could be argued that it is incomplete since only two of the six linear conditions of the rule $\Delta J = 1$ are tested. But this is not the case, as we shall explain below.

It would be difficult to draw the 6-dimensional projection on $\mathcal{C}_P$ of the polarization domain $\mathcal{D}$, but it is very easy to draw the three projections on the 2-dimensional planes $X_1Y_1, X_2Y_2, X_3Y_3$; it is the triangle $BCD$ and the two circles, cf. table 2e,

$$X_2^2 + Y_2^2 \leqslant \tfrac{9}{40} , \qquad X_3^2 + Y_3^2 \leqslant \tfrac{1}{4} , \tag{26}$$

respectively. We explain in appendix C how to compute them. We also prove in this appendix the following result. If the two linear conditions of the tetrahedron are satisfied (i.e. the projection $\mathcal{C}_D$ of the experimental point falls on the segment $AB$), angular momentum and parity conservation imply

$$X_2^2 + Y_2^2 \leqslant \tfrac{9}{160} , \qquad X_3 = Y_3 = 0 . \tag{27}$$

This result is easy to understand qualitatively. Since the projection of $\mathcal{C}_T$ on the 2-plane $\mathcal{C}_{P1}$ spanned by $X_1Y_1$ is on the boundary (point $A = Q$) of the projection (triangle $BCD$) of $\mathcal{D}$, the 17-dimensional plane $\mathcal{C}_\perp$, orthogonal to $\mathcal{C}_{P1}$, at $A = Q$ is tangent to $\mathcal{D}$. Its contact with $\mathcal{D}$ is much more than one point, but it is much smaller than $\mathcal{D}$ so it has a smaller projection than $\mathcal{D}$ on the two other 2-planes $X_2Y_2$ and $X_3Y_3$.

If the projection of the experimental point on the tetrahedron falls on a point $E_D$ in the segment $AQ$, we can even use this information to decrease the limit of $X_2^2 + Y_2^2$. As we prove in appendix C if $l$ is the linear coordinate of $E_D$ on $AQ$,

$$l = \overline{AE_D}/\overline{AQ} , \tag{28}$$

then one has, cf. table 2f,

$$X_2^2 + Y_2^2 \leqslant \tfrac{9}{160}\, l^2 . \tag{29}$$

## 5. Experimental test of the rule $\Delta J = 1$

We have gathered from the published literature a set of 50 experimental points contained in 16 different papers. The nature of the reaction, the beam energy, the number of bins in momentum transfer and the references of all these papers are given in table 3. It may seem totally irrelevant to mix all these data. However in order to show that, for all reactions of type (1), the experimental results are strongly in favor of the selection rule $\Delta J = 1$, we have plotted, in fig. 2, the 50 experimental points altogether. The clustering of the data along the lines or at the points predicted by the rule is impressive.

Table 3
Experimental data on joint polarization for reactions of type $0^-\frac{1}{2}^+ \to 1^-\frac{3}{2}^+$

| Reaction | Beam momentum (in GeV/c) |
|---|---|
| (a) $\pi^+p \to \rho^0\Delta^{++}$ | 3.–4.[G]6, 3.7[M]8, 5.[A]1, 8.[B]1, 11.7[I]4, 13[P]6 |
| (b) $\to \omega\Delta^{++}$ | 3.7[M]4, 5.[A]1, 8.[B]1, 11.7[L]3, 13[P]5 |
| (c) $K^+p \to K^{*0}\Delta^{++}$ | 1.4–2.2[K]1, 1.7[N]1, 2.1–2.7[F]1, 2.5–3.2[E]1, 3.1[H]1, 4.3–5[O]1, 5.[C]1 |
| (d) $K^-n \to K^{*0}\Delta^-$ | 3.[D]1 |
| (e) $K^-p \to \rho^-\Sigma^{*+}$ | 3.9–4.6[J]1 |
| $\to \phi\Sigma^{*0}$ | 3.9–4.6[J]1 |

The capital letter in [ ] gives the reference below, and the following figure indicates the number of experimental points (for different bins in momentum transfer).

[A] Bonn-Durham-Nijmegen-Paris-Strasbourg-Turin Collaboration, K. Bockmann et al., Phys. Letters 28B (1968) 72.
[B] Aachen-Berlin-CERN Collaboration, M. Aderholz et al., Nucl. Phys. B8 (1968) 485.
[C] W. de Baere et al., Nuovo Cimento 61A (1969) 400.
[D] SABRE Collaboration, B. Haber et al., Nucl. Phys. B17 (1970) 289.
[E] G.S. Abrams et al., Phys. Rev. D1 (1970) 2433.
[F] A. Borg, Thèse de doctorat 3ème cycle, 1970, Université de Paris.
[G] D. Brown et al., Phys. Rev. D1 (1970) 3053.
[H] K. Buchner et al., Nucl. Phys. B29 (1971) 381.
[I] R.O. Maddock et al., Nuovo Cimento 5A (1971) 445.
[J] M. Aguilar-Benitez et al., Phys. Rev. D6 (1972) 29.
[K] S.C. Loken et al., Phys. Rev. D6 (1972) 2346.
[L] D. Evans et al., Nucl. Phys. B51 (1973) 205.
[M] K.W.J. Barnham et al., Phys. Rev. D7 (1972) 1384.
[N] A. Berthon et al., Nucl. Phys. B63 (1973) 54.
[O] G. Dehm et al., Nucl. Phys. B71 (1974) 52.
[P] J.A. Gaidos et al., Nucl Phys. B72 (1974) 253.

For a more detailed study, it is better to consider separately each experiment for each reaction. Since it was not possible to present twenty-one figures in this paper we have restricted ourselves to six. Five of them correspond to experiments with the largest number of bins in momentum transfer. Experiments [M] and [P] of table 3 have been performed at the present extreme values of energy (3.7 GeV and 13 GeV for the $\pi$ beam) and for both reactions $\pi^+p^+ \to \rho^0\Delta^{++}$ or $\omega^0\Delta^{++}$ (figs. 3 and 6). The $\Delta J = 1$ rule is very well verified in all four cases. All experimental points are grouped near $T_P$ defined in eq. (24). Furthermore each figure has also (at the same scale) the plot proposed in ref. [1]. This tetrahedron plot shows very interesting features. Indeed if one were only interested in the $\Delta J = 1$ rule, it would be sufficient to use the three projections on the 2-planes $X_1Y_1, X_2Y_2, X_3Y_3$. The plots of figs. 3 to 8 use

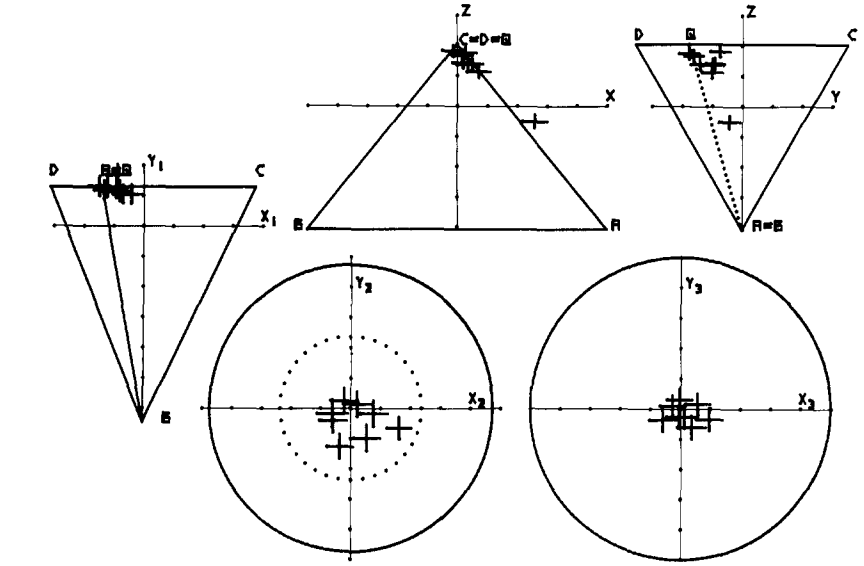


Fig. 3. Test of the rule $\Delta J = 1$ for the experiments $\pi^+ p \to \rho^0 \Delta^{++}$ ref. [M] of table 3 at 3.7 GeV/$c$. The agreement is excellent Except for the bin with larger $|t|$ (for which another mechanism takes place), all the other experimental points are near the point $Q$, which represents pure unnatural parity exchange or one-pion exchange, see ref. [18].

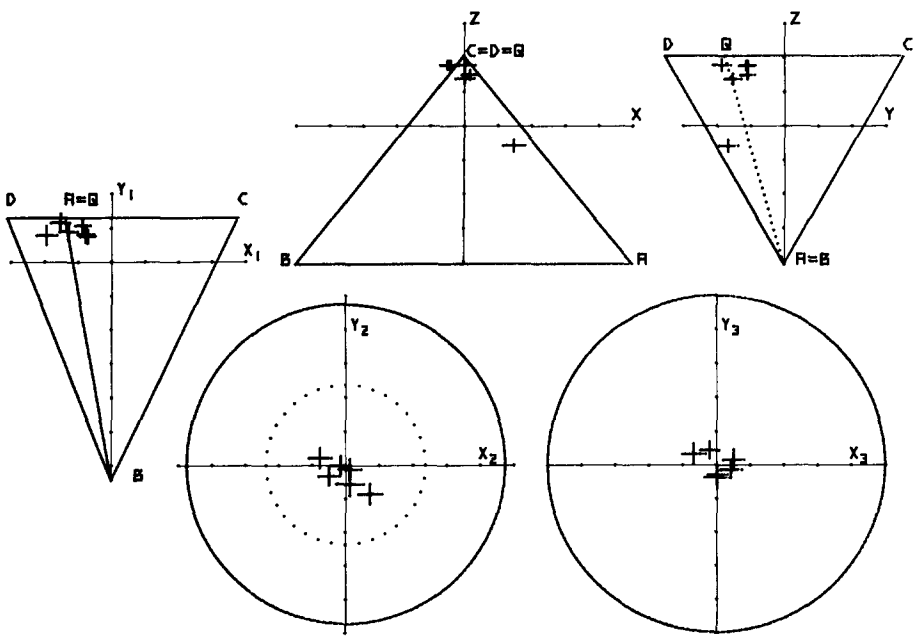


Fig. 4. Test of the rule $\Delta J = 1$ for the experiment $\pi^+ p \to \rho^0 \Delta^{++}$ ref. [P] of table 3 at 13 GeV/$c$. The data is remarkably similar to that of fig. 3 at 3.7 GeV/$c$.

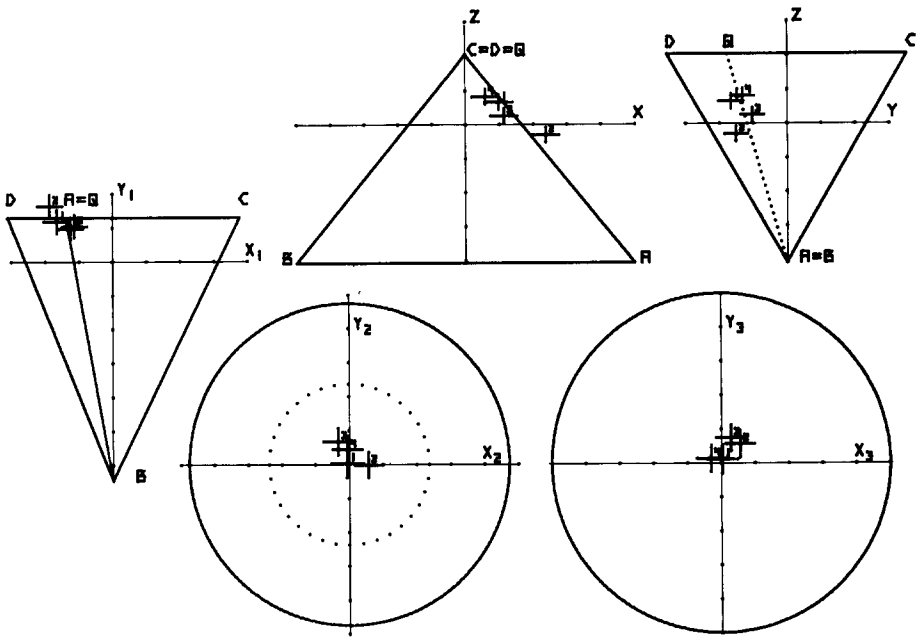


Fig. 5. Test of the rule $\Delta J = 1$ for the experiment $\pi^+ p \to \omega^0 \Delta^{++}$ ref. [M] of table 3, at 3.7 GeV/$c$. The agreement is excellent. Since one-pion exchange is impossible, the data lies on the segment $AQ$ farther from $Q$ than the corresponding $\rho^0$ data at the same energy (fig. 3). The height of the experimental point in the upper triangles represents the mixture of unnatural (top) and natural (bottom) parity exchange.

seven dimensions, and the degree of freedom left by the rule $\Delta J = 1$ is the position along the segment $AQ$. Using, as at the end of sect. 4, the parameter $l$ for the linear coordinate on $AQ$ ($l = 0$ in $A$, $l = 1$ in $Q$), $l$ measures the mixture of unnatural ($Q$) to natural ($A$) parity exchange in this reaction [18]. From this point of view, $\rho^0$ and $\omega^0$ production are very different. We refer to the caption of figs. 3 to 6 for more details. Fig. 7 shows the whole published data (seven points from seven different experiments) for the reaction $K^+ p \to K^{*0} \Delta^{++}$; it also satisfies the $\Delta J = 1$ rule. Finally fig. 8 shows the data on $\pi^+ p \to \rho^0 \Delta^{++}$ at the same energy as that of fig. 4. The comparison between the two data shows the usefulness of a polarization plot.

To conclude, the very simple tetrahedron plot that we proposed in 1973 is not only a fairly complete test of the rule $\Delta J = 1$ for the present data with rather large bins in $t$, but it also yields the physical parameter $l$ (e.g. for experiment [J] with a ~4 GeV $K^-$ beam on proton, $l$ is 0.2 for $\rho^- \Sigma^{*+}$ production and 0.7 for $\Phi \Sigma^{*0}$ production).

Of course more complete polarization plots could be performed, even in this complicated case with 19 measurable polarization parameters. This paper and ref.

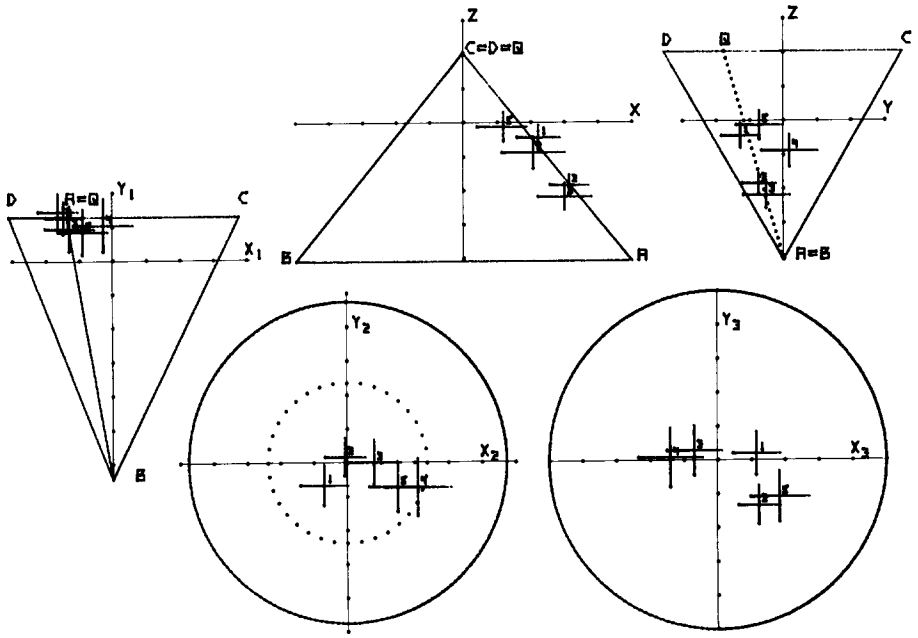


Fig. 6. Test of the rule $\Delta J = 1$ for the experiment $\pi^+ p \to \omega^0 \Delta^{++}$ ref. [P] of table 3, at 13 GeV/$c$. Although the errors are larger than at 3.7 GeV/$c$ (fig. 5) the data presents the same features, but with more natural parity exchange. We recall that only the upper half of the segment $AQ$ is allowed by angular momentum and parity conservation in the forward and backward directions. We remark that as $|t|$ increases the experiment data start from the middle of $AQ$ (point 1), go down (points 2 and 3) and return to the upper half of $AQ$ in the backward direction (5). Similar oscillations but of smaller amplitude can be observed in fig. 5.

[1b] are examples of what can be done. We can supply the same or more detailed plots for the different experiments of table 3.

## Appendix A

### *Polarization space and polarization domain*

Polarization is described by a hermitian, positive, trace one matrix $\rho$, the density matrix. The $n \times n$ hermitian matrices form an $n^2$-dimensional space $\mathcal{E}_{n^2}$, with the natural Euclidean scalar product

$$(\rho_1, \rho_2) = \operatorname{tr} \rho_1 \rho_2 \ . \tag{A.1}$$

Positive hermitian matrices (i.e., with non-negative eigenvalues) form a convex cone $\mathcal{C}$ in $\mathcal{E}_{n^2}$ and the trace one matrices from a hyperplane $\mathcal{E}_N$ ($N = n^2 - 1$) called the

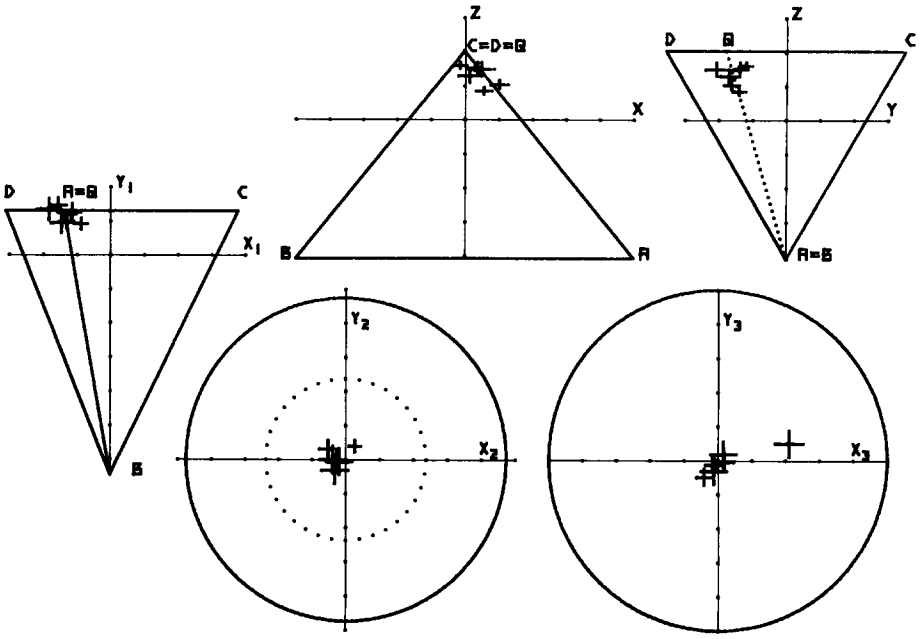


Fig. 7. Test of the rule $\Delta J = 1$ for the reactions $K^+p \to K^{*0}\Delta^{++}$ for seven experiments, refs. [N, K, F, E, H, O, C] of table 3, at energies between 2 and 5 GeV/$c$, and for integrated values of $t$. So the forward direction has a bigger influence. The data is remarkably precise and well clustered, except for one aberrant projection in $(X_3, Y_3)$ incompatible with angular momentum and parity conservation. (It might be a misprint in the paper of ref. [H]').

*polarization space.* The density matrices are in the intersection of $\mathcal{C}$ and $\mathcal{E}_N$. They form a convex domain $\mathcal{D}$ called the *polarization domain.*

An orthonormal basis is defined in $\mathcal{E}_N$ if the coordinates $p_i$, $i = 1, ..., N$ of a density matrix $\rho$ with respect to this basis are such that

$$(\rho, \rho) = \operatorname{tr} \rho^2 = \frac{1}{n} + \sum_{i=1}^{N} (p_i)^2 \ . \tag{A.2}$$

For instance, consider the multipole expansion of the $(2j + 1) \times (2j + 1)$ density matrix of a spin-$j$ particle

$$\rho_\nu^\mu = \sum_{L,M} \sqrt{\frac{2j+1}{2L+1}} \langle j\mu LM | j\nu \rangle T_M^L \ . \tag{A.3}$$

One has

$$\operatorname{tr} \rho^2 = \frac{1}{2j+1} + \sum_{L=1}^{2j} [(T_0^L)^2 + \sum_{M>0} 2|T_M^L|^2] \ . \tag{A.4}$$

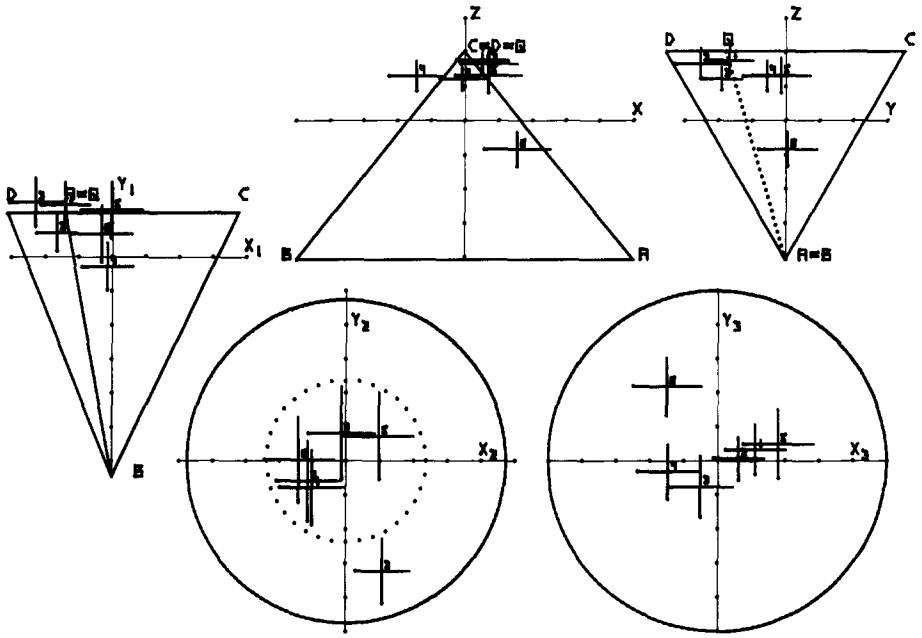


Fig. 8. Test of the rule $\Delta J = 1$ for the reaction $\pi^+ p \to \rho^0 \Delta^{++}$ at 3 to 4 GeV/$c$, ref. [G] of table 3. It is the same reaction at the same energy as fig. 3. The comparison of the two figures shows that this data is less precise and much more scattered. The possibility of such direct comparisons is a by-product of this type of geometrical test.

Therefore the multipole parameters $T_0^L$ and $\sqrt{2}$ Re $T_M^L$, $\sqrt{2}$ Im $T_M^L$ $(M > 0)$ are the coordinates of $\rho$ with respect to an orthonormal basis. The boundary of $\mathcal{D}$ is formed of positive matrices with rank less than their dimension $n$. Thus the domain $\mathcal{D}$ can be explicitly defined in terms of a set of parameters $p_i$ as the convex domain containing the origin $\rho_0$ of $\mathcal{E}_N$ and bounded by the surface with equation $\det \rho = 0$.

In most high-energy experiments it is not possible to observe $\rho$ completely: only some of the parameters $p_i$ (e.g. the multipole parameters with $L$ even) can be measured. In our geometrical language, this corresponds to observing only the orthogonal projection $\rho_{ob}$ of $\rho$ on a subspace $\mathcal{E}_{ob}$. The domain allowed for $\rho_{ob}$ is the projection $\mathcal{D}_{ob}$ of $\mathcal{D}$ on $\mathcal{E}_{ob}$. If the intersection of $\mathcal{D}$ by $\mathcal{E}_{ob}$ and its projection on $\mathcal{E}_{ob}$ are equal, the plane $\mathcal{E}_{ob}$ is called an equatorial plane of $\mathcal{D}$ and then $\rho_{ob}$ must be positive. But if $\mathcal{E}_{ob}$ is not an equatorial plane, $\rho_{ob}$ is not necessarily positive. This is the case for the plane $\mathcal{E}_{19}$ considered in the main text [17].

For the most usual experimental situations, the domain $\mathcal{D}_{ob}$ was first described in ref. [19] for spin 1 and in ref. [20] for spin $\frac{3}{2}$. A more detailed study of the material in this appendix can be found in refs. [8–10].

## Appendix B

*Constraints predicted by the rule $\Delta J = 1$*

Table 1c gives the expressions of the 19 observables in terms of the 12 complex transversity amplitudes. Using the relations (22) implied by the selection rule $\Delta J = 1$, these expressions read

$$\sigma = |a|^2 + 2|b|^2 + 2|b'|^2 + 2|c|^2 + 2|c'|^2 ,$$

$$T_{00}^{02} = (12)^{-1/2}[-|a|^2 + |b|^2 + |b'|^2 + |c|^2 + |c'|^2]/\sigma ,$$

$$T_{00}^{22} = (24)^{-1/2}[2|a|^2 + |b|^2 + |b'|^2 + |c|^2 + |c'|^2]/\sigma ,$$

$$T_{00}^{20} = (6)^{-1/2}[-|a|^2 + |b|^2 + |b'|^2 + |c|^2 + |c'|^2]/\sigma , \tag{B.1}$$

$$T_{02}^{02} = (2)^{-1/2}[c\bar{b}' + b\bar{c}']/\sigma , \qquad T_{22}^{22} = (\tfrac{3}{2})^{1/2} c\bar{c}'/\sigma ,$$

$$T_{02}^{22} = \tfrac{1}{2}[c\bar{b}' + b\bar{c}']/\sigma , \qquad T_{2-2}^{22} = (\tfrac{3}{2})^{1/2} c\bar{c}'/\sigma ,$$

$$T_{20}^{22} = \tfrac{1}{2}[c\bar{b} + b'\bar{c}']/\sigma , \qquad T_{11}^{22} = (\tfrac{3}{16})^{1/2}[a\bar{c}' + c\bar{a}]/\sigma ,$$

$$T_{20}^{20} = [c\bar{b} + b'\bar{c}']/\sigma , \qquad T_{1-1}^{22} = (\tfrac{3}{16})^{1/2}[a\bar{b} + b'\bar{a}]/\sigma . \tag{B.2}$$

By inspection of these expressions one readily gets six linear constraints between the observables

$$T_{00}^{20} = \sqrt{2}\, T_{00}^{02} = \frac{1}{\sqrt{6}} - 2T_{00}^{22} ,$$

$$T_{20}^{20} = 2T_{20}^{22} , \qquad T_{02}^{02} = \sqrt{2}\, T_{02}^{22} . \tag{B.3}$$

In addition the observables satisfy non-linear constraints. To simplify their writing we define the new set of observables

$$A \equiv |a|^2/\sigma = \tfrac{1}{3}[1 - (24)^{1/2} T_{00}^{20}] ,$$

$$B \equiv (c\bar{b}' + b\bar{c}')/\sigma = T_{20}^{20} ,$$

$$B' \equiv (c\bar{b}' + b\bar{c}')/\sigma = (2)^{1/2} T_{02}^{02} ,$$

$$C \equiv c\bar{c}'/\sigma = (\tfrac{2}{3})^{1/2} T_{22}^{22} ,$$

$$D \equiv (a\bar{c}' + c\bar{a}')/\sigma = (\tfrac{16}{3})^{1/2} T_{11}^{22} ,$$

$$E \equiv b'\bar{b}/\sigma = (\tfrac{2}{3})^{1/2} T^{22}_{2-2} ,$$

$$F \equiv (a\bar{b} + b'\bar{a})/\sigma = (\tfrac{16}{3})^{1/2} T^{22}_{1-1} . \qquad \text{(B.4)}$$

The observables are independent of the overall phase of the amplitudes, thus we may assume that the amplitude $a$ is real positive. Then it is straightforward to perform the "amplitude reconstruction" i.e., to compute the amplitudes in terms of the observables, cf. ref. [14]. One gets

$$a = \sqrt{\sigma A} ,$$

$$\bar{b}, b' = \frac{1}{2} \sqrt{\frac{\sigma}{A}} (F \pm \sqrt{F^2 - 4AE}) ,$$

$$c, \bar{c}' = \frac{1}{2} \sqrt{\frac{\sigma}{A}} (D \pm \sqrt{D^2 - 4AC}) . \qquad \text{(B.5)}$$

The modulus of these amplitudes is related to the differential cross section $\sigma$ by eq. (B.1). This implies the constraint

$$A^2 + |D|^2 + |D^2 - 4AC| + |F|^2 + |F^2 - 4AE| = A , \qquad \text{(B.6)}$$

which is of degree 8 in the observables. Furthermore replacing the amplitudes by their values (B.5) in the relations

$$\sigma B = \tfrac{1}{2}(c + \bar{c}')(\bar{b} + b') + \tfrac{1}{2}(c - \bar{c}')(\bar{b} - b') ,$$

$$\sigma B' = \tfrac{1}{2}(c + \bar{c}')(\bar{b}' + b) + \tfrac{1}{2}(c - \bar{c}')(b' - b) , \qquad \text{(B.7)}$$

one gets (2 complex = 4 real) cubic constraints,

$$AB^2 - BDF + CF^2 + D^2 E + 4ACE = 0 ,$$

$$AB'^2 - B'D\bar{F} + C\bar{F}^2 + D^2 \bar{E} - 4AC\bar{E} = 0 . \qquad \text{(B.8)}$$

We remark that the observables are invariant for the simultaneous exchange $b \Leftrightarrow \bar{b}'$ and $c \Leftrightarrow \bar{c}'$. Indeed once an arbitrary convention is made for $\bar{b}, b'$, eq. (B.8) resolves the ambiguity for $c, \bar{c}'$.

## Appendix C

*Projection of $\mathcal{D}$ on $X_2 Y_2$ and $X_3 Y_3$*

In this appendix we establish formulae (26), (27) and (29).

(1) We first study the projections of $\mathcal{D}_A$, the non-convex amplitude domain.

Using tables 1c and 2b we find

$$X_3 + iY_3 = \langle d|a\rangle/2\sigma \,. \tag{C.1}$$

With Schwartz inequality we obtain

$$|X_3 + iY_3| \leqslant \sqrt{\Delta_A/2\sigma}\sqrt{\Delta_B/2\sigma} \,. \tag{C.2}$$

Since the sum of the two factors on the right side satisfies

$$\frac{\Delta_A}{2\sigma} + \frac{\Delta_B}{2\sigma} \leqslant 1 \,, \tag{C.3}$$

the maximum of $|X_3 + iY_3|$ is obtained for $\Delta_A = \Delta_B = 1/4\sigma$, $\Delta_C = \Delta_D = 0$;

$$|X_3 + iY_3| \leqslant \tfrac{1}{2} \qquad \text{i.e.} \; X_3^2 + Y_3^2 \leqslant \tfrac{1}{4} \,. \tag{C.4}$$

Similarly, we find from tables 1c and 2b

$$X_2 + iY_2 = \frac{1}{\sqrt{10}} (\langle f|e\rangle - 3\langle c|b\rangle)/2\sigma \,. \tag{C.5}$$

Hence

$$|X_2 + iY_2| \leqslant \frac{1}{2\sigma}\frac{1}{\sqrt{10}} (|\langle f|e\rangle| + 3|\langle c|b\rangle|) \leqslant \frac{1}{2\sqrt{10}} \frac{\Delta_D + 3\Delta_C}{2\sigma} \,. \tag{C.6}$$

The maximum is obtained for $\Delta_A = \Delta_B = \Delta_D = 0$; $\Delta_C = 2\sigma$,

$$|X_2 + iY_2| \leqslant \frac{3}{2\sqrt{10}} \qquad \text{i.e.} \; X_2^2 + Y_2^2 \leqslant \tfrac{9}{40} \,. \tag{C.7}$$

These two projections (C.4) and (C.7) of $\mathcal{D}_A$ are circles: they are convex; so they are also the projections of the convex hull $\hat{\mathcal{D}}_A$ of $\mathcal{D}_A$. This establishes formula (26).

Let us assume that the rule $\Delta J = 1$ is satisfied, i.e. the relations (22) hold, e.g. $d = d' = 0$; this implies $\langle d|a\rangle = 0$ in (C.1) so

$$X_3 = Y_3 = 0 \,. \tag{C.8}$$

This result was already established in ref. [21] (their appendix) and in ref. [22]. The former reference makes for its own data a test similar to that of the tetrahedron. However, this data is not published so we do not use it in this paper.

From the relations in (22) involving $b, c, e, f$ we obtain $\Delta_D = 3\Delta_C$; with this constraint the maximum of the bound in (C.6) is obtained for $\Delta_A = \Delta_B = 0$, so $\Delta_C = \frac{1}{2}\sigma$, $\Delta_D = \frac{3}{2}\sigma$ and

$$X_2^2 + Y_2^2 \leqslant \tfrac{9}{160} \,. \tag{C.9}$$

When the relation (22) holds, only the amplitude $a$ corresponds to a natural parity exchange (indeed $\mu = 0$ in $A_\lambda^{\mu\mu'}$ of table 1b, cf. ref. [18]); the other amplitudes $b$, $b', c, c'$ correspond to unnatural parity exchange ($\mu = \pm 1$ in $A_\lambda^{\mu\mu'}$). Hence we can define

$$1 - I = \frac{\langle a|a\rangle}{2\sigma} = \frac{\Delta_A}{2\sigma} . \tag{C.10}$$

If $I$ is fixed, the maximum of the bound in (C.6) is obtained for $\Delta_B = 0$ but $\Delta_A = 2\sigma(1 - I)$ so $\Delta_C = \frac{1}{2}I\sigma$, $\Delta_D = \frac{3}{2}I\sigma$ and

$$X_2^2 + Y_2^2 \leqslant \frac{9I^2}{160} . \tag{C.11}$$

(ii) Although (C.8) and (C.9) are identical to (27) and (C.11) to (29), they have only been established assuming the rule $\Delta J = 1$ is satisfied. We now prove (27) and (29) assuming only angular momentum and parity conservation and that the projection on $\mathcal{E}_D$ of the experimental data falls in a point $E_D$ of the segment $AQ$.

The joint polarization density matrix $\rho$ for spin 1 and $\frac{3}{2}$ particles is a $12 \times 12$ matrix and has therefore 143 observables. If these particles are produced in a reaction $0 + \frac{1}{2} \to 1 + \frac{3}{2}$ with unpolarized target, parity conservation implies 72 linear relations among them. In a transversity basis, with a suitable reordering of lines and columns, $\rho$ is a direct sum of two $6 \times 6$ positive matrices. The projection of $\rho$ on the symmetry 35-plane $\mathcal{E}_{35}$ of observables defined by "$L_1 + L_2$ even" is $\rho_{(35)} = \rho'' \otimes \rho''^{\mathrm{T}}$ (ref. [17] as simple extension of ref. [18]). The observable $\rho_{\mathrm{ob}}$ is the projection of $\rho_{(35)}$ on the 19-dimensional polarization space $\mathcal{E} \subset \mathcal{E}_{35}$ of observables defined by "$L_1$ even and $L_2$ even". It has still the structure $\rho = \rho' \otimes \rho'^{\mathrm{T}}$ but $\mathcal{E}$ is not an equatorial plane so $\rho'$ is not necessarily positive: we can only use the fact that $\rho'$ is an orthogonal projection of the positive $\rho''$.

Any principal $2 \times 2$ submatrix $\rho_{[i,j]}$

$$\rho_{[i,j]} = \begin{pmatrix} \rho_{ii} & \rho_{ij} \\ \overline{\rho_{ij}} & \rho_{jj} \end{pmatrix}$$

of the positive matrix $\rho''$ is positive. Let us consider the three submatrices

$$i = 1, \tfrac{3}{2}, \quad j = -1, \tfrac{3}{2}, \qquad \rho_{\mathrm{I}} = \tfrac{1}{2}\begin{pmatrix} D_D - \alpha_D & \overline{Z_D} \\ Z_D & D_D + \alpha_D \end{pmatrix} , \tag{C.12a}$$

$$i = 1, -\tfrac{1}{2}, \quad j = -1, -\tfrac{1}{2}, \qquad \rho_{\mathrm{II}} = \tfrac{1}{2}\begin{pmatrix} D_C - \alpha_C & \overline{Z_C} \\ Z_C & D_C + \alpha_C \end{pmatrix} , \tag{C.12b}$$

$$i = 0, \tfrac{1}{2}, \quad j = 0, -\tfrac{3}{2}, \qquad \rho_{\mathrm{III}} = \tfrac{1}{2}\begin{pmatrix} D_A & \overline{Z_3} \\ Z_3 & D_A \end{pmatrix} . \tag{C.12c}$$

The coordinates of these matrices in the observable space $\mathcal{C}$ are

$$D_X = \Delta_X/4\sigma\,, \qquad \sum_X D_X = \tfrac{1}{2}\,, \qquad (X = A, B, C, D)\,, \tag{C.13}$$

$$\frac{1}{\sqrt{10}}(Z_D - 3Z_C) = X_2 + iY_2\,, \tag{C.14}$$

$$2Z_3 = X_3 + iY_3\,. \tag{C.15}$$

The coordinates $\alpha_C$, $\alpha_D$ and $\sqrt{\frac{1}{10}}\,(Z_D + 3Z_C)$ are orthogonal to $\mathcal{C}$ in $\mathcal{C}_{35}$. Since they are not observable they are called ghost parameters [17]. The positivity of the $\rho_{\mathrm{I,II,III}}$ matrices in (C.12) implies

$$D_X \geqslant 0\,, \qquad X = A, B, C, D\,; \tag{C.16}$$

moreover $\rho_{\mathrm{III}} \geqslant 0$ is equivalent to

$$(X_3^2 + Y_3^2) = 4|Z_3|^2 \leqslant 4D_A D_B\,, \tag{C.17}$$

which is identical to (C.2).

Similarly, $\rho_{\mathrm{I}} \geqslant 0$, $\rho_{\mathrm{II}} \geqslant 0$ are equivalent to $|Z_D| \leqslant D_D$, $|Z_C| \leqslant D_C$, so

$$|X_2 + iY_2| \leqslant \frac{1}{\sqrt{10}}\,(|Z_D| + 3|Z_C|) \leqslant \frac{1}{\sqrt{10}}\,(D_D + 3D_C)\,, \tag{C.18}$$

which is (C.6). So we have proven again (27). In $\mathcal{C}_{\mathrm{D}}$, the equation of the segment $AQ$ is given by

$$D_B = 0 \qquad (\text{face } ACD)\,, \tag{C.19a}$$

$$D_D = 3D_C\,. \tag{C.19b}$$

Eq. (C.19a) combined with (C.17) yields $X_3 = Y_3 = 0$. Eqs. (C.19b) and (C.10) yield

$$\frac{1}{\sqrt{10}}\,(D_D + 3D_C) = \frac{3l}{4\sqrt{10}}\,, \tag{C.20}$$

so, with (C.18)

$$X_2^2 + Y_2^2 \leqslant \tfrac{9}{160}\,l^2\,. \tag{C.21}$$

The dotted circle in figs. 3 to 8 corresponds to the maximum $l = 1$. We have already emphasized the physical meaning of $l$. We add here, without proof, that for forward or backward reactions, angular momentum and parity conservation require [8]

$$\tfrac{1}{2} \leqslant l \leqslant 1\,. \tag{C.22}$$

## References

[1] M.G. Doncel, P. Minnaert and L. Michel, The polar angle distribution in joint decay of spin-1 and $\frac{3}{2}$ resonances, CERN/D.Ph.II/Phys. 73-39, Communication to 2nd Aix-en-Provence Conf. on elementary particles; Test of models and polarization effects: The quark model, 3rd Int. Winter Meeting on fundamental physics, ed. J. Diaz Bejarano and M.G. Doncel (Instituto de Estudios Nucleares, Madrid).
[2] L Stodolsky and J J. Sakurai, Phys. Rev. Letters 11 (1963) 90.
[3] C. Itzykson and M. Jacob, Nuovo Cimento 49A (1967) 909
[4] J.L. Friar and J.S. Trefil, Nuovo Cimento 49A (1967) 842.
[5] A. Białas and K. Zalewski, Nucl. Phys B6 (1968) 465.
[6] Kupczynski, Acta Phys. Pol. B1 (1970) 301.
[7] A. Kotanski, Ecole Internationale de la Physique des Particules Elémentaires, Herceg-Novi 1970, Institut B. Kidric, Belgrade.
[8] M.G. Doncel, L. Michel and P. Minnaert, Polarization density matrix, PTB reports 35, 37, 44, Laboratoire de Physique Théorique, Université de Bordeaux I; Matrices densité de polarization, Ecole d'Eté de Gif-Sur-Yvette 1970, ed R. Salmeron (Laboratoire de Physique, Ecole Polytechnique, Paris).
[9] P. Minnaert, The polarization domain, in Particle physics, Les Houches 1971, ed. C. de Witt and C. Itzykson (Gordon and Breach, New York).
[10] M.G. Doncel, L. Michel and P. Minnaert, Nucl. Phys. B38 (1972) 477.
[11] M. Daumens, G. Massas, L. Michel and P. Minnaert, Nucl. Phys. B53 (1973) 303.
[12] M. Daumens, G. Massas and P. Minnaert, Systematic analysis of sequential decays in canonical and helicity frames, PTB, Lab. de Phys. Théorique, Université Bordeaux I.
[13] P. Minnaert, Spin tests from particle decays, in 3rd Int. Winter Meeting on fundamental physics, ed. J. Diaz Bejarano and M.G. Doncel (Instituto de Estudios Nucleares, Madrid).
[14] M.G. Doncel, L. Michel and P. Minnaert, Fortsch. Phys. 24 (1976) 259 and CERN/D.Ph. II/Phys. 74-7.
[15] M. Simonius, Phys. Rev. Letters 19 (1967) 279.
[16] J.T. Donohue, M. Hontebeyrie and Ch. Meyers, Nucl. Phys. B109 (1976) 91.
tion $\pi N \to \rho\Delta$, PTB 65, Lab. de Phys. Theor., Université Bordeaux I.
[17] M.G. Doncel, L. Michel and P. Minnaert, unpublished.
[18] M.G. Doncel, P. Merry, L. Michel, P. Minnaert and K.C. Wali, Phys. Rev. D7 (1973) 815.
[19] P. Minnaert, Phys. Rev 151 (1966) 1306.
[20] M.G. Doncel, Nuovo Cimento 52A (1967) 617.
[21] L. Lyons, U. Karshon, Y. Eisenberg, G. Mikenberg, S. Pitluck, E.E. Ronat, A. Shapira and G. Yekutieli, Nucl. Phys. B85 (1975) 165.
[22] T. Jaroszewicz, Acta Phys. Pol. B4 (1973) 21.